

AD-A042 752

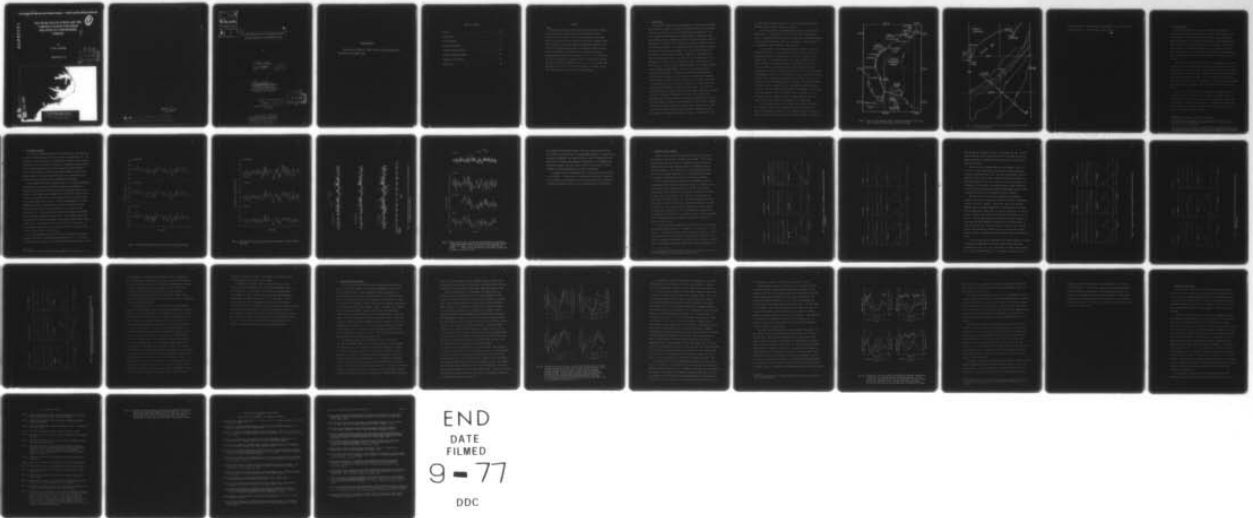
NEVADA UNIV RENO DEPT OF ELECTRICAL ENGINEERING
SEA LEVEL FLUCTUATIONS OFF THE CAROLINA COASTS AND THEIR RELATI--ETC(U)
MAY 76 D A BROOKS
NCSU-CMCS-77-6

F/G 8/3

UNCLASSIFIED

NL

1 of 1
AD
A042752



END
DATE
FILMED
9 - 77
DDC

AD A 042752

SEA LEVEL FLUCTUATIONS OFF THE
CAROLINA COASTS AND THEIR
RELATION TO ATMOSPHERIC
FORCING

0

[Handwritten signature]

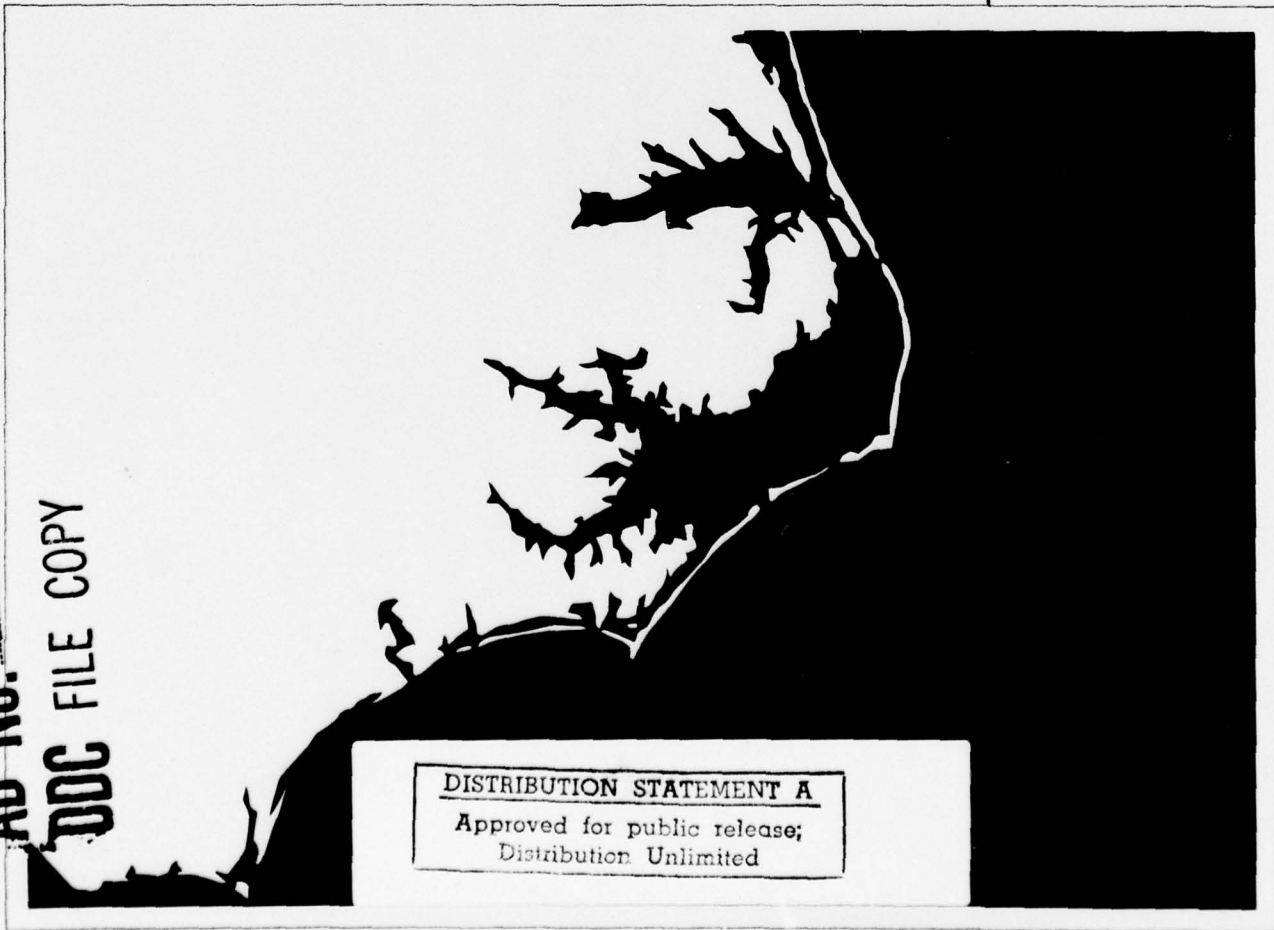
By

DAVID A. BROOKS

REPORT NO. 77-6

DDC
RECEIVED
AUG 5 1977
D
[Handwritten initials]

AD No. _____
DDC FILE COPY



DISTRIBUTION STATEMENT A

Approved for public release;
Distribution Unlimited

410322

North Carolina State Univ, Raleigh.
Center for Marine and Coastal Studies.

ACCESSION for	
NTIS	White Section <input checked="" type="checkbox"/>
DDC	Butt Section <input type="checkbox"/>
UNANNOUNCED <input type="checkbox"/>	
JUSTIFICATION	
Per Htr. on file	
BY	
DISTRIBUTION/AVAILABILITY CODES	
Dist.	AVAIL. and/or SPECIAL
A	

6 SEA LEVEL FLUCTUATIONS OFF THE CAROLINA COASTS
AND THEIR RELATION TO ATMOSPHERIC FORCING.

by

10 DAVID A. BROOKS
11 May 1977
12 45p.

9 Final Report, to the
University Research Committee
for Project Number 627
North Carolina State University
Raleigh, North Carolina

14 NCSU-CMCS-
Report No. 77-6

DDC
RECEIVED
AUG 5 1977
D

410 322

DISTRIBUTION STATEMENT A
Approved for public release;
Distribution Unlimited

43

ACKNOWLEDGMENTS

This study was funded by a grant from the Faculty Research and Professional Development Fund.

Table of Contents

Abstract	iii
Introduction	1
Data processing	6
Time domain analysis	9
Frequency domain analysis	15
Multiple regression models	26
Summary and conclusions	34
References	36

ABSTRACT

Atmospheric pressure and wind stress fluctuations are strongly coupled to sea level fluctuations along the Carolina coasts at periods of 2.5 to 3.5 days. Sea level fluctuations in this band exhibit high coherence over a horizontal separation exceeding 500 km. Phase difference calculations indicate southward propagation of the sea level fluctuations from Beaufort to Wilmington, North Carolina; the data considered are insufficient to conclusively determine propagation direction south of Wilmington. The 2.5 - 3.5 day period sea level fluctuations are consistent with a theoretically expected first mode, barotropic continental shelf wave. It is concluded that continental shelf waves forced by the atmosphere contribute to the shelf and slope water circulation off North Carolina.

1. Introduction

It is commonly observed that the movements of coastal and continental shelf waters are related to atmospheric variables such as the local wind. Over the last decade or so it has gradually been realized that a class of low (subinertial) frequency wave motions known as continental shelf waves (CSW's) provide a physical mechanism by means of which the energy of atmospheric fluctuations can be focused into energetic continental shelf and slope water motions. Low frequency sea level fluctuations associated with these motions are often observed to be coherent over hundreds of kilometers in the alongshore direction. Examples of the existence of oceanic fluctuations in this class, detected as low frequency sea level fluctuations, are given for the Australian coasts by Hamon (1962), for the western U.S. coast by Mooers and Smith (1968), for the North Carolina coast by Mysak and Hamon (1969), and for the east Florida coast by Brooks and Mooers (1977). The details of atmosphere-ocean coupling processes and the degree of their importance to the total circulation over continental shelves are still a matter of active debate, but there is little doubt that CSW's universally account for at least part of the low frequency variability of coastal and shelf waters. The currently mounting pressure for prudent coastal and shelf water management strategies calls for an improved understanding of how CSW's are forced by the atmosphere and how they influence the circulation patterns over the shelf. This study examines linkages between atmospheric forces and low frequency sea level fluctuations along the Carolina coasts, taking account of the coherent relationship between surface atmospheric pressure and winds. The results of the study are discussed in light of CSW parameters such

as period and wavelength expected for the North Carolina shelf region (Brooks, 1976a; hereafter referred to as B76).

The Carolina shelf is the northeastward arm of the South Atlantic Bight, Fig. 1. The Cape Hatteras region of the North Carolina shelf may be a singularly important zone of CSW generation, since the departure of the Gulf Stream from the coast there represents an abrupt change in the continental shelf waveguide characteristics.

In the presence of the background relative vorticity of the Gulf Stream off Cape Fear, low mode stable barotropic CSW's are expected to propagate southward, in opposition to the advective tendency of the Stream, (B76). The zero group speed, first mode CSW (likely to be forced by rapidly traveling atmospheric cold fronts) has a period of about three days and an alongshore wavelength of about 20 km; its southward phase speed is thus 140 km day^{-1} (160 cm s^{-1}). The period and wavelength were found to be quite sensitive to the details of the current profile, because the upstream propagation speed of the wave is of the same order as the downstream speed of the current. The predicted along-shore wave velocity component (v) has a maximum value near the coast, a node near the shelf break (approximately 100 km offshore of Cape Fear), and decays rapidly seaward of the shelf break. The predicted cross shelf wave velocity component (u) has a maximum value near the shelf break, and decreases seaward and shoreward of the shelf break.

The right-handed, "natural" coordinate system used in B76 and in this study has been rotated clockwise 55.6 degrees, such that the x axis is approximately orthogonal to the isobaths off Cape Fear, Fig. 2, line A-B; this is the line along which Richardson, Schmitz, and Niiler

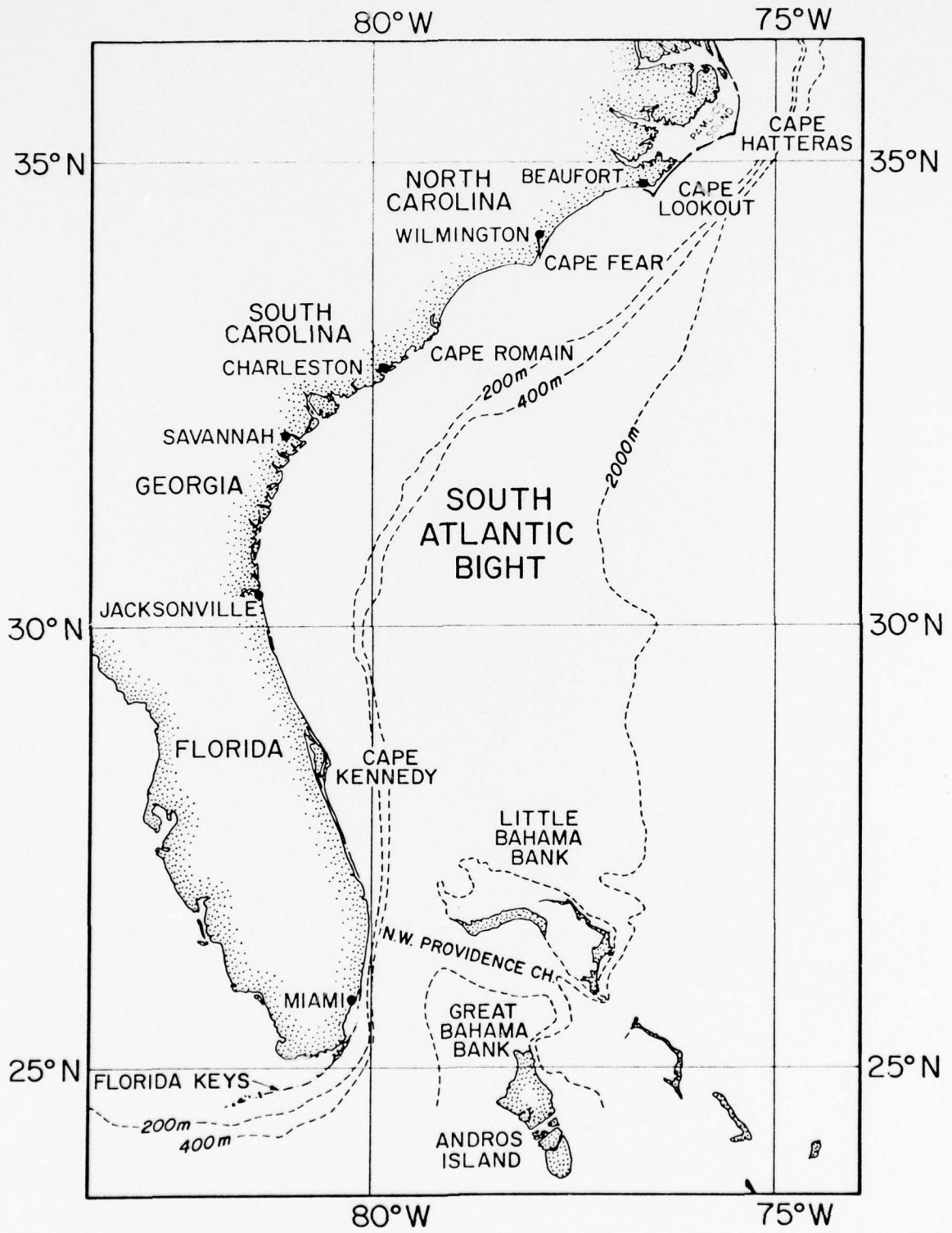


Fig. 1 Map of South Atlantic Bight, showing locations of tide gauge and atmospheric station data used in the study.

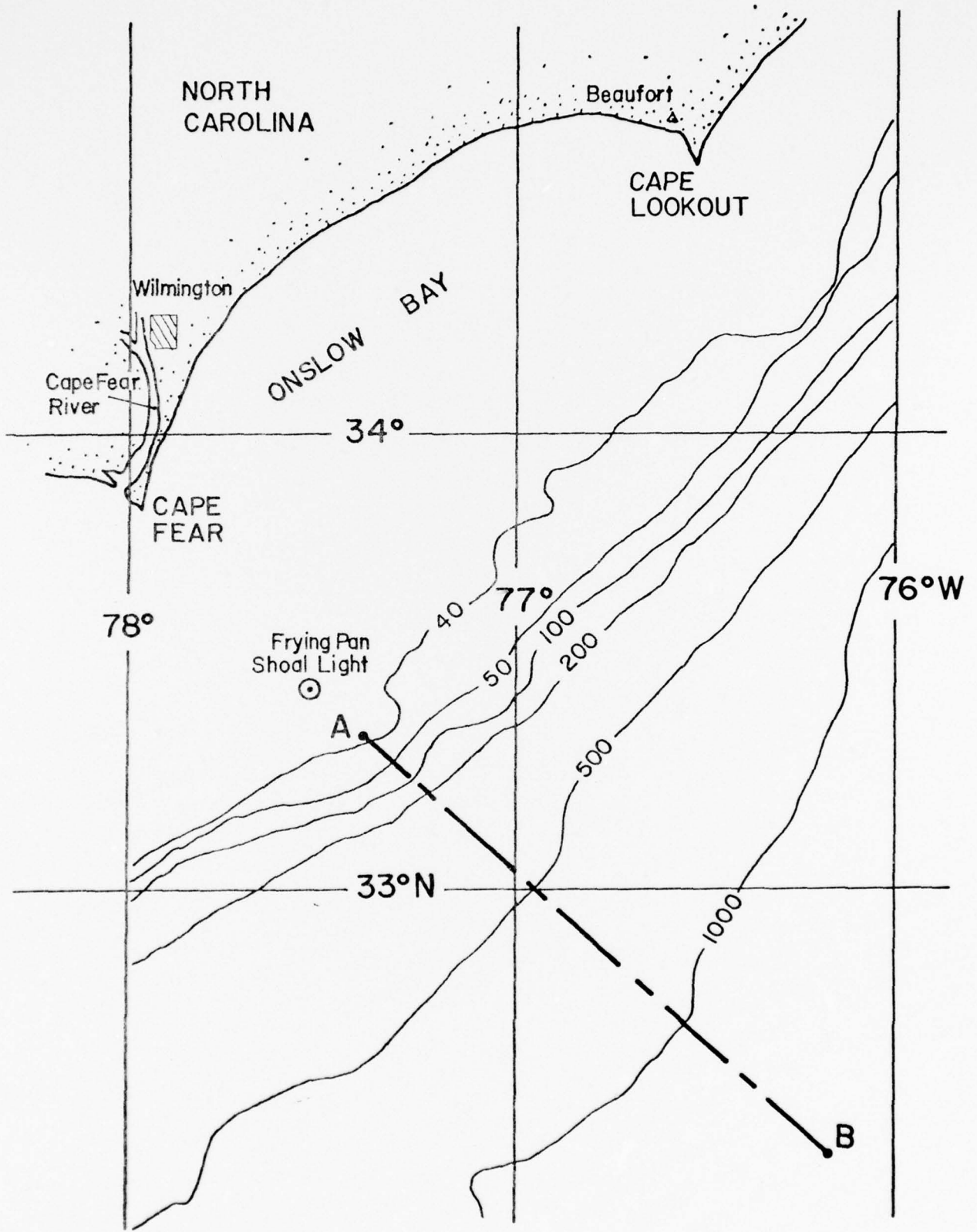


Fig. 2 Onslow Bay continental shelf topography, showing coordinate system orientation.

(1969) performed a two-month dropsonde measurement of the Gulf Stream's velocity structure. The coordinate origin is point A.

2. Data Processing

The data analyzed are from coastal sea level (tide gauge) and meteorological stations located in Figs. 1 and 2. Hourly values of sea level height for 1974 were obtained from National Ocean Survey, NOAA, Rockville, Maryland, for stations at Beaufort (BFT) and Wilmington (WIL), North Carolina; and at Charleston (CHS), South Carolina. Three-hourly values of surface wind speed, wind direction, and atmospheric pressure for 1974 were obtained from the National Climatic Center, NOAA, Asheville, North Carolina for stations at Cape Hatteras (HAT)¹, North Carolina, WIL, and CHS.

The raw data set chosen for this study is a small subset of the total amount of coastal atmospheric and tide gauge data available in the South Atlantic Bight from the year 1974. The stations BFT and WIL were selected to compare with a similar study of earlier data from stations near those locations, Mysak and Hamon (1969). CHS was included as a third station because of its availability at the beginning of the study², and to increase the maximum available alongshore separation distance (BFT-CHS) to about 500 km.

The sea level data were low pass filtered³ to attenuate the daily and semidaily tides and inertial fluctuations (the inertial period at Cape Fear is 21.5 hours). The envelope of the "two-day low pass" filter energy response function is shown in Fig. 3. Attenuation at diurnal and higher frequencies is greater than 10^6 . After filtering, the sea level data were resampled at 8-hour intervals.

¹Atmospheric data were not available at Beaufort.

²It was subsequently learned that a tide gauge at Avon, N. C. (near Cape Hatteras) was operational during 1974; the data from Avon will be included in a subsequent study.

³A Lanczos filter taper with 241 weights (10 days in length) was used. Thus five days (120 data points) are lost from the beginning and from the end of the raw time series. The low pass filtered time series start at 0000 hrs

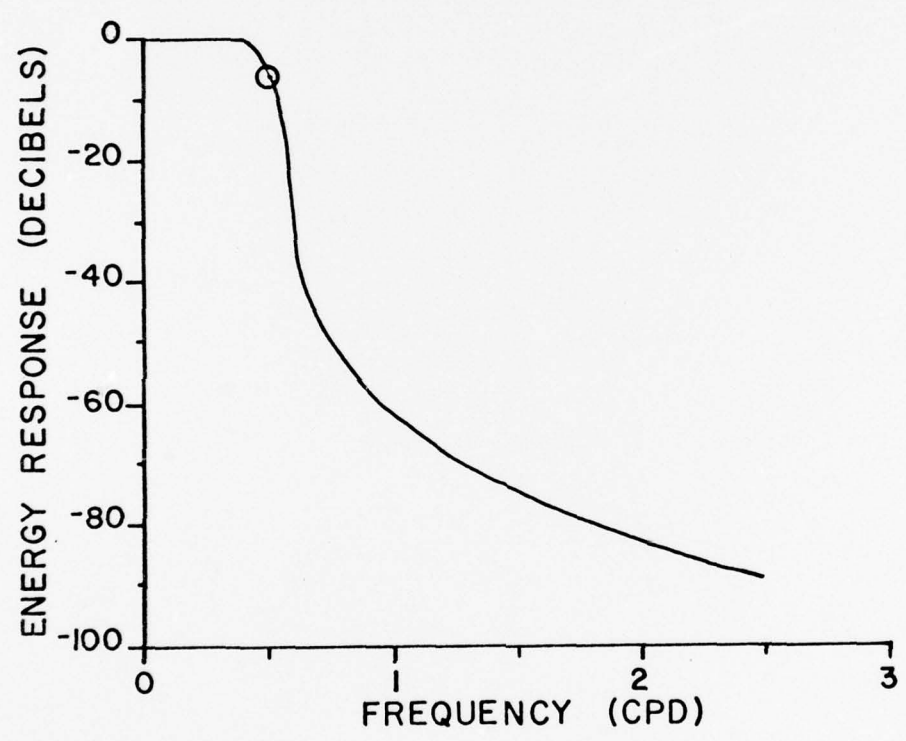


Fig. 3 Low pass filter energy response envelope function. Attenuation at 1 CPD is 10^6 .

Three-hourly wind stress vector components in the rotated coordinate system were computed from the raw wind speed and direction data, with the positive vector sense in the direction toward which the wind blows. The stress components were computed using a quadratic drag law with the drag coefficient $C_D = 1.5 \times 10^{-3}$. The wind stress components and atmospheric pressure time series were low pass filtered, using a filter with the response characteristics shown in Fig. 3. The atmospheric data were then subsampled at 9-hour intervals and linearly interpolated to 8-hour intervals to be commensurate with the sea level data.

The analyses were conducted for two subsets of the filtered 1974 data. A 120-day subset (6 Jan to 6 May) was chosen to reflect late winter-early spring atmospheric forcing conditions (i.e., to emphasize the relative importance of cold front passages over the Carolina shelf during that period, compared to the distinctively different character of summer atmospheric conditions). A 292-day subset, 6 Jan to 25 Oct, was chosen to permit an approximate comparison with the 1953 analysis period used by Mysak and Hamon (1969) (2 Jan to 4 Sept); and to provide coverage of a period in which "winter-like" and "summer-like" atmospheric forcing conditions were given roughly equal time weights.

Extensive use is made of spectrum analysis. Except where noted otherwise, all frequency domain calculations were made by Fourier transforming tapered correlation functions. The effective spectrum bandwidth is 0.0667 cycles per day (CPD), with 16 (39) degrees of freedom for the 120 (292) day subset. "Coherence squared" has been abbreviated to "coherence" in the text; all confidence intervals and significance tests are referred to the 95% level.

3. Time Domain Analysis

The filtered atmospheric pressure fluctuations show a high degree of visual correlation between the CHS, WIL, and HAT stations (Fig. 4)⁴. The similarity is apparent even for relatively small amplitude, short period fluctuations (e.g., days 42-46), indicating a horizontal coherence length scale of the pressure field much greater than the CHS-HAT Separation distance (about 500 km). The large horizontal coherence distance presumably reflects the synoptic meteorological scales (thousands of km) associated with mid-latitude winter atmospheric disturbances.

The alongshore wind stress component (Fig. 5) also shows considerable correlation over the CHS-HAT separation distance, but variations in intensity and structure between stations are more apparent than in the pressure. The largest stress component ($+2.2 \text{ dyne cm}^{-2}$) occurred at HAT at day 54; this "event" can be clearly identified at WIL and CHS, where it was progressively less intense. A vector representation, or "stick" diagram, of the wind stress shows the clockwise rotation of the wind field usually associated with the passage of a cold front over the station (Fig. 6). Again, there is much similarity between the stations, with the largest intensity occurring at HAT. The strongest winds tend to align with the coastal topography, as indicated by near-vertical wind stress vectors. Wind stress "reversals" (defined by a sign change of the alongshore component), most clearly noted at HAT, occurred on time scales of several days to several weeks.

Sea level responded to the major wind stress events in the manner expected from coastal upwelling and downwelling (Fig. 7). For example, the wind stress events with a strong northeastward component that occurred

⁴The origin of all time domain figures is 0000 hrs 01 January 1974.

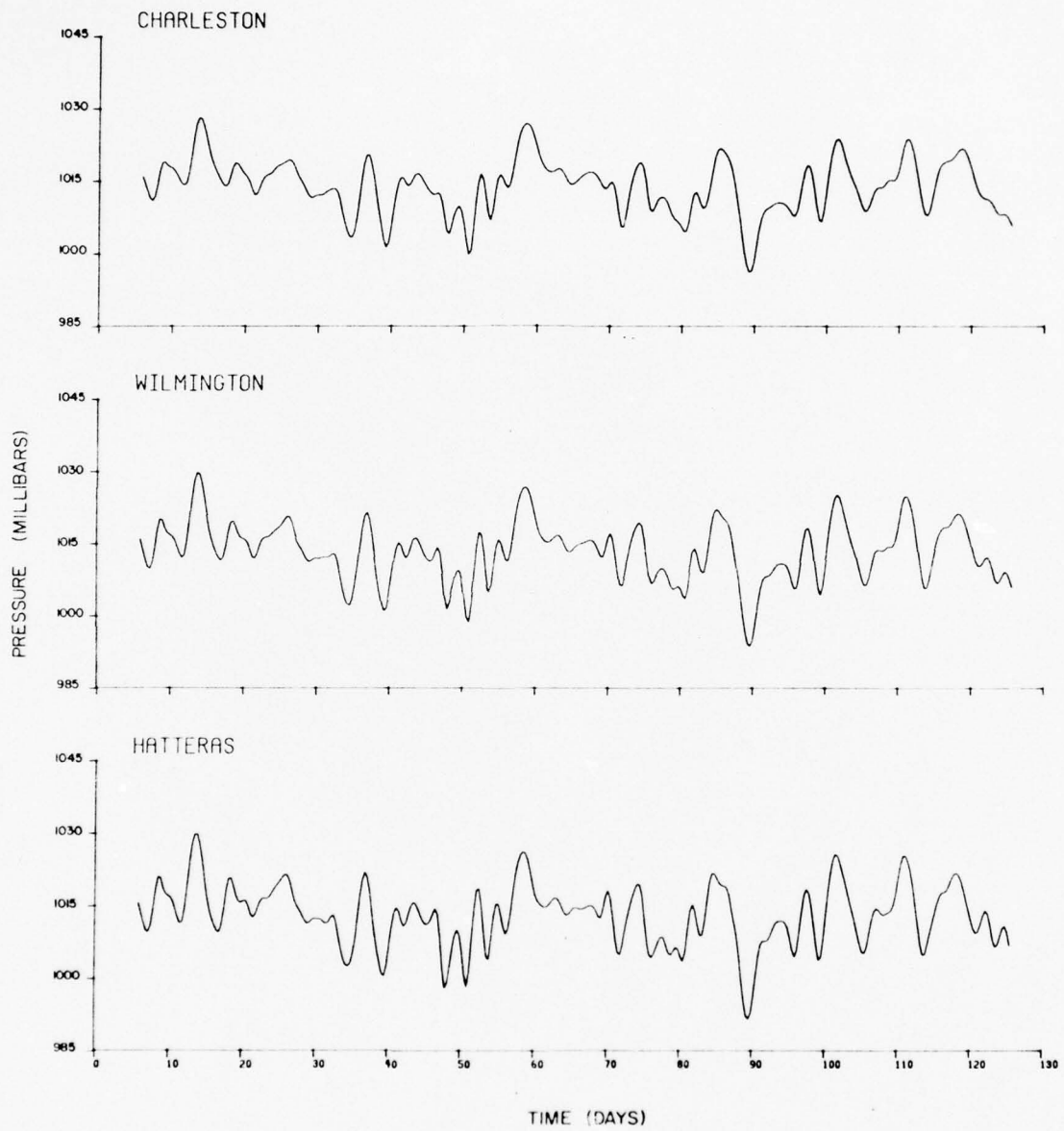


Fig. 4 Filtered atmospheric pressure at three coastal stations.

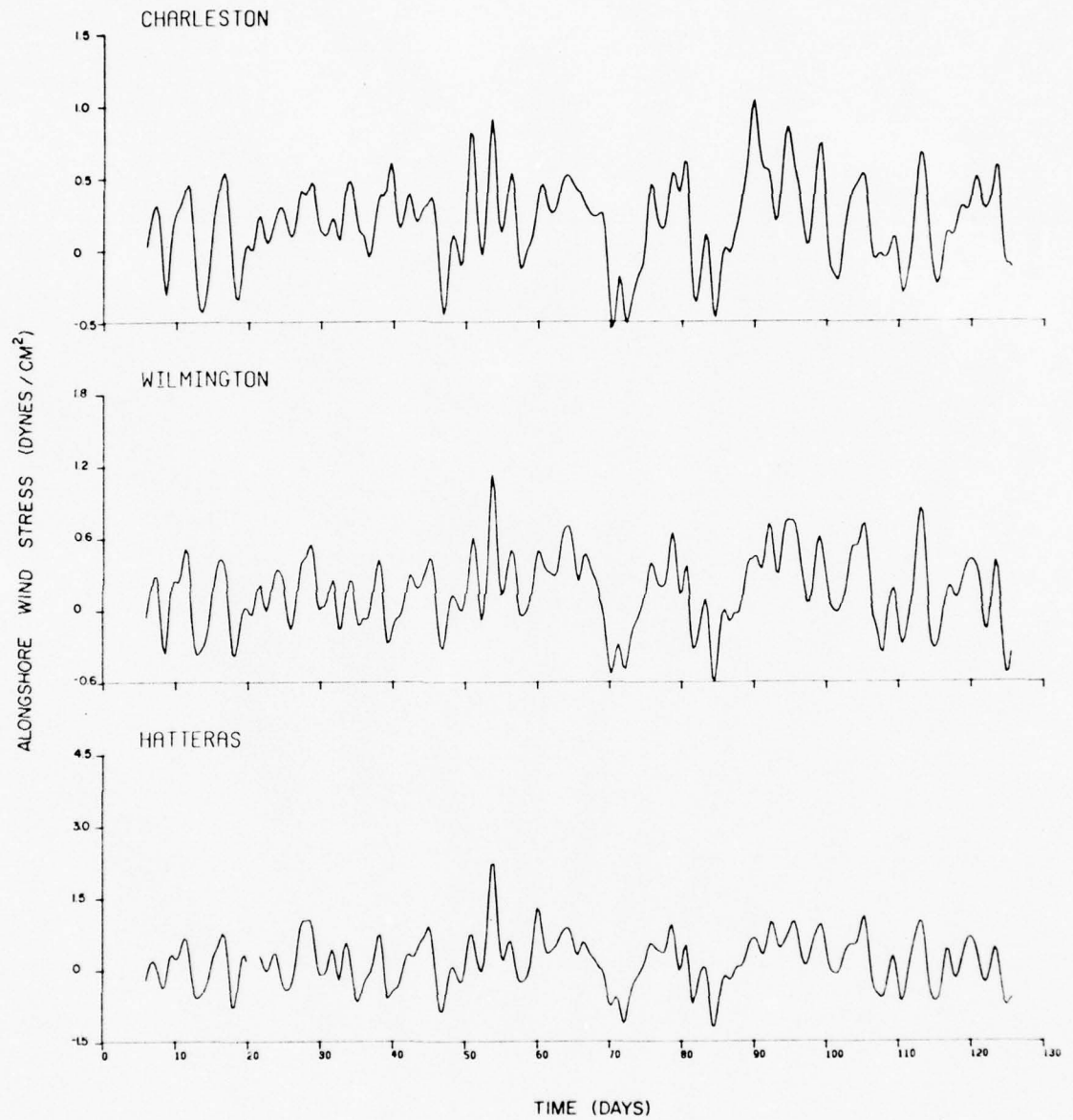


Fig. 5 The filtered along shore wind stress component at three coastal stations.

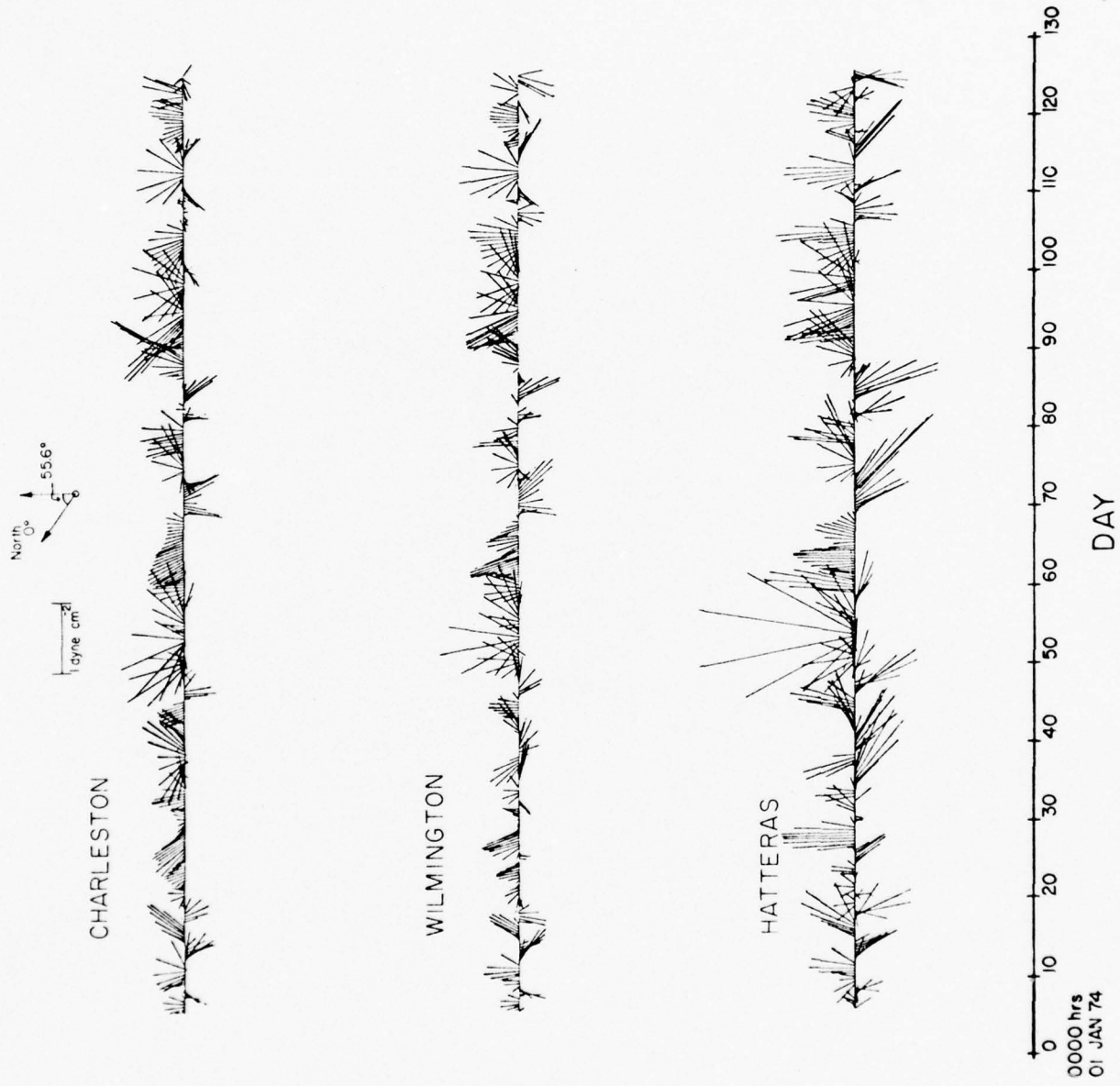


Fig. 6 Filtered wind stress vectors in the rotated coordinate system for three coastal stations.

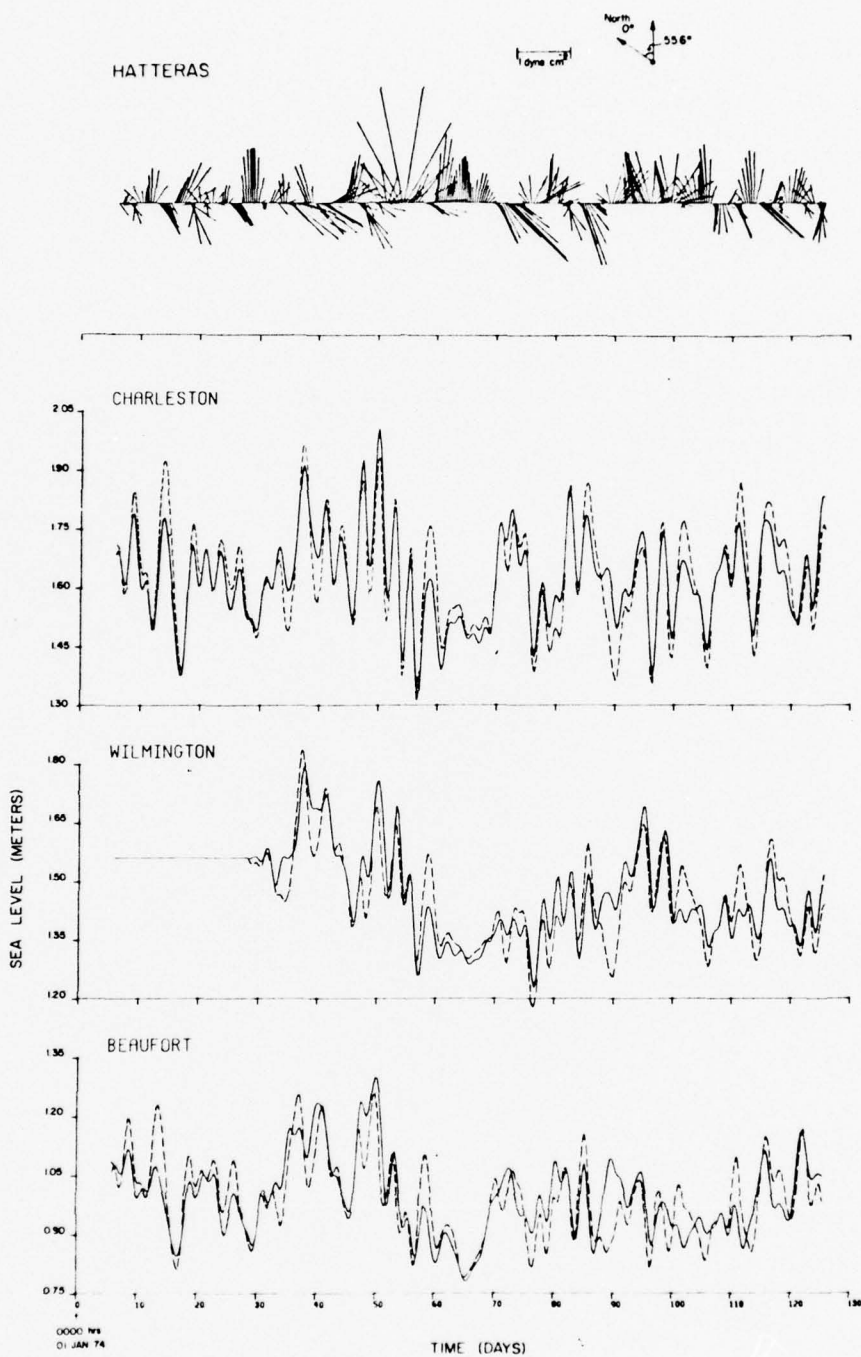


Fig. 7 Wind stress vectors at Cape Hatteras and their relation to unadjusted (solid lines) and barometrically adjusted (dashed lines) sea level. Static adjustment is accomplished by adding 1.01 cm from sea level for each local atmospheric pressure increase of 1 mb.

during days 53-55 and 60-88 caused a total sea level set-down of about 55 cm at BFT, consistent with an offshore Ekman transport of surface waters and coastal upwelling. The abrupt reversal at day 70 to persistent wind stress with a southwestward component during days 70 - 74 (downwelling-favorable) produced a sea level set-up of about 30 cm at BFT. Similar responses of different magnitudes occurred at CHS and WIL.

A prominent sea level oscillation with a several day period occurred at all stations. In most cases, the several day oscillation is enhanced in the barometrically adjusted sea level curves (dashed line), indicating a selective atmospheric pressure ocean coupling process at this period.

4. Frequency domain analysis

In this section, the coherence and phase between various pairs of atmospheric and sea level variables are discussed. First, atmospheric pressure and wind stress are examined; second, sea level is examined; and third, some linkages between the atmosphere and sea level are examined. All calculations in this section were carried out for only one input function, i.e. no correction has been made for coherent relationships with other possible input functions.

The large horizontal coherence scale of atmospheric pressure fluctuations deduced from the time domain results is confirmed by the high coherence (~ 0.9) between pressure at HAT and CHS, separated approximately 500 km (Fig. 8B). The pressure fluctuations are nearly in phase for all frequencies in the range 0 to 0.5 cycles per day (CPD), indicating that synoptic scale pressure disturbances arrive at HAT and CHS at nearly the same time. The largest phase lag⁵ occurred at a period of about 3 days, with HAT lagging CHS by several hours. Both wind stress components at WIL were significantly coherent with the pressure for periods of 2.5 to 10 days, with the cross shelf (along shelf) component exhibiting a quadrature (antiphase) tendency with respect to the pressure.

The coherence between unadjusted sea level records for the 120 day period shows rather sharp peaks at periods of 2.5 - 3.5 and 7 - 30 days (Fig. 9). The highest coherence (0.96) occurred at a period of 3 days in the calculation between BFT and WIL, confirming the time domain observation of prominent several day oscillations at those stations. Surprisingly, the coherence at periods longer than 10 days is higher between

⁵ In all frequency-domain figures, positive phase angles mean that the first-named variable leads the second-named variable.

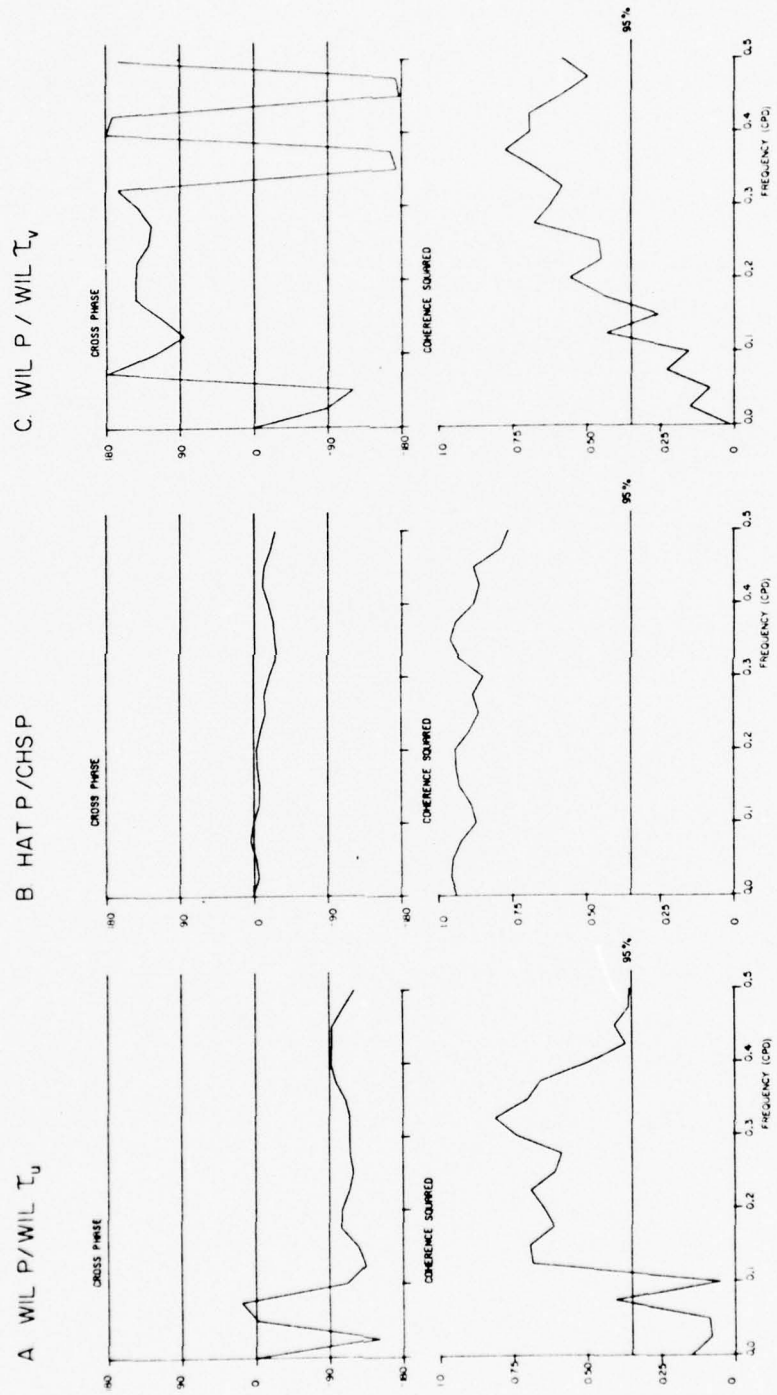


Fig. 8 Coherence and phase for atmospheric pressure and wind stress components.

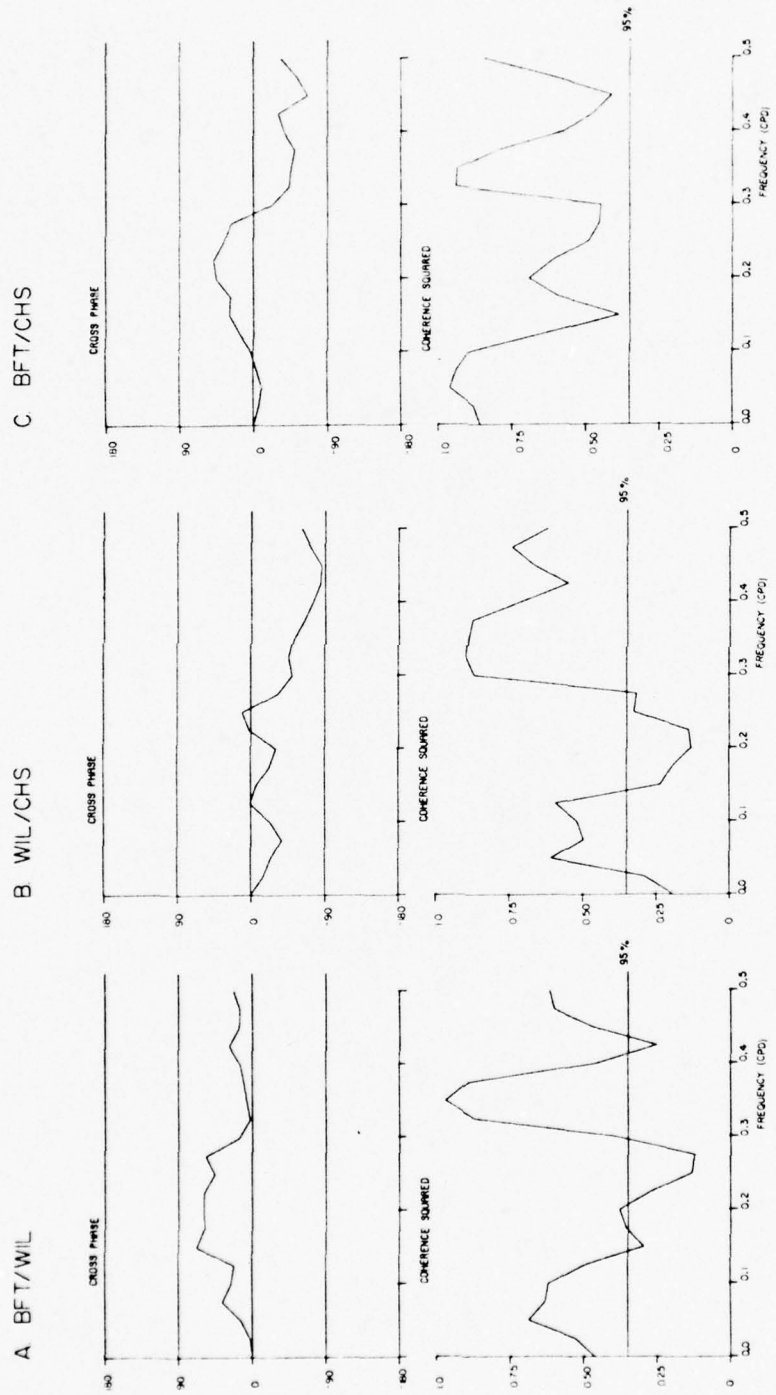


Fig. 9 Coherence and phase for unadjusted 120-day sea level records.

BFT and CHS (the "extrema" stations) than between WIL (the "central" station) and BFT or CHS; this may reflect the fact that the WIL tide gauge is located a considerable distance upstream from the mouth of the Cape Fear river.

Clearly resolved coherence peaks are also apparent in the 2.5 - 3.5 and 7 - 30 day bands when the multi-season, 292-day unadjusted records are considered (Fig. 10). The phase relationships, which are similar for both record lengths, generally indicate fluctuations at BFT leading those at WIL. On the other hand, the fluctuations at CHS lead those at WIL and BFT in the coherent bands, possibly reflecting a static sea level oscillation traveling northeastward along the coast in phase with synoptic-scale atmospheric pressure systems.

When the sea level is statically adjusted for atmospheric pressure (for each mb of pressure increase at the nearest atmospheric station, 1.01 cm is added from the sea level), the coherence between stations increases significantly in the spectral gap between the two peaks noted earlier (Fig. 11, 120 day record; Fig. 12, 292 day record). However, the highest coherence values consistently occur in the 2.5 - 3.5 day band, even after the static correction is made. In that band, the phase indicates fluctuations at BFT leading those at WIL by 0.3 to 0.4 day. The phase results in the 2.5 to 3.5 day band indicate CHS leading WIL and BFT by about 0.3 and 0.1 days, respectively; the lead is somewhat smaller than in the cases of unadjusted sea level.

The cross shelf and the along shelf wind stress components are both consistently coherent with the 120-day record adjusted sea level fluctuations in the 2.5 - 3.5 day band (Fig. 13, cross-shelf component; Fig. 14, along shelf component). The coherence is generally low for

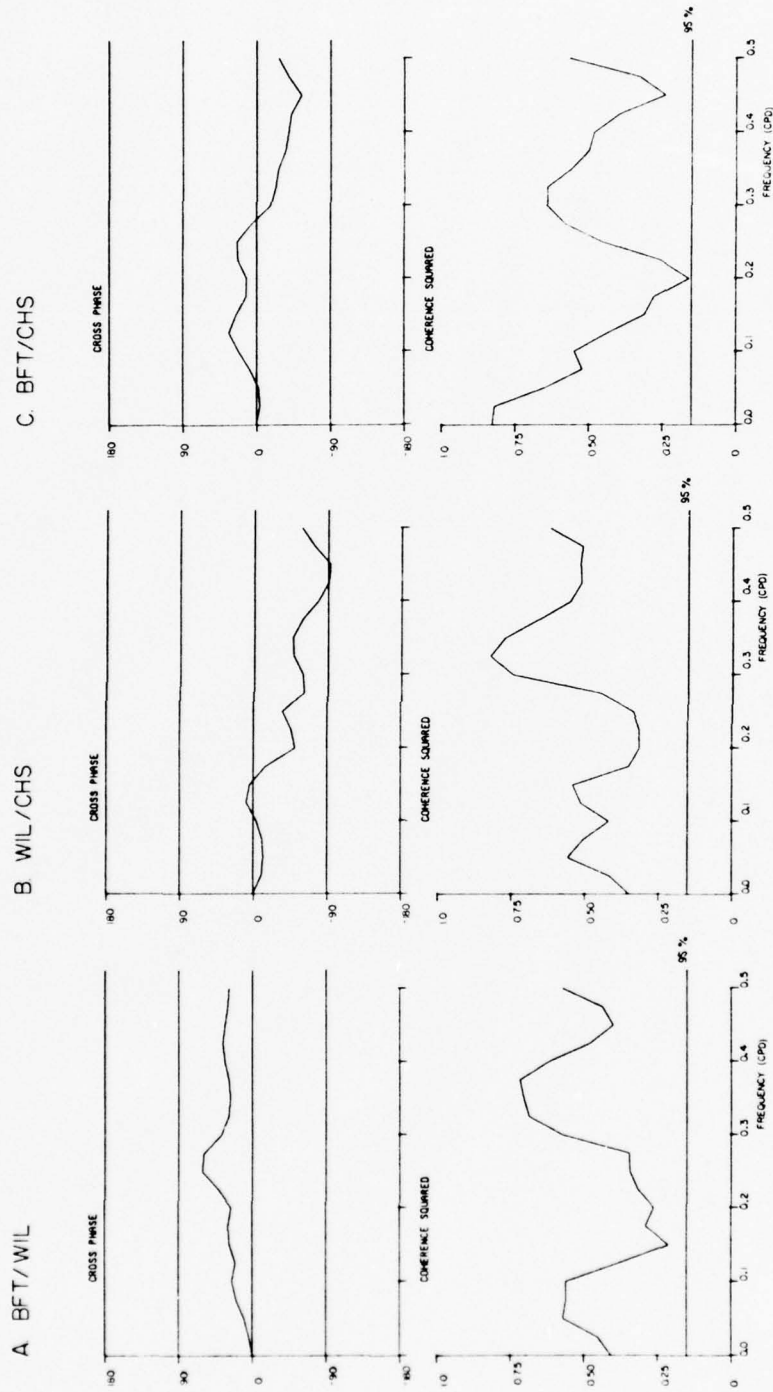


Fig. 10 Coherence and phase for unadjusted 292-day sea level records.

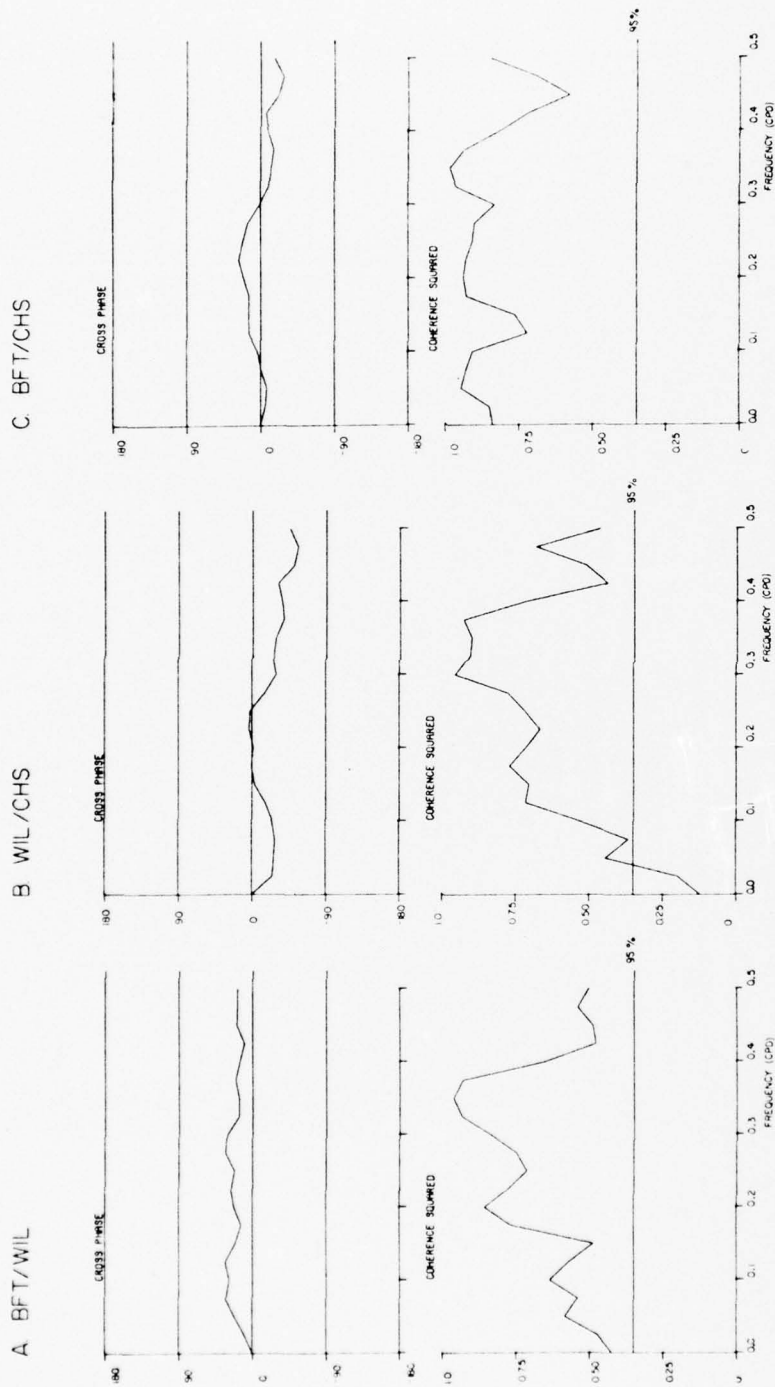


Fig. 11 Coherence and phase for barometrically adjusted 120-day sea level records.

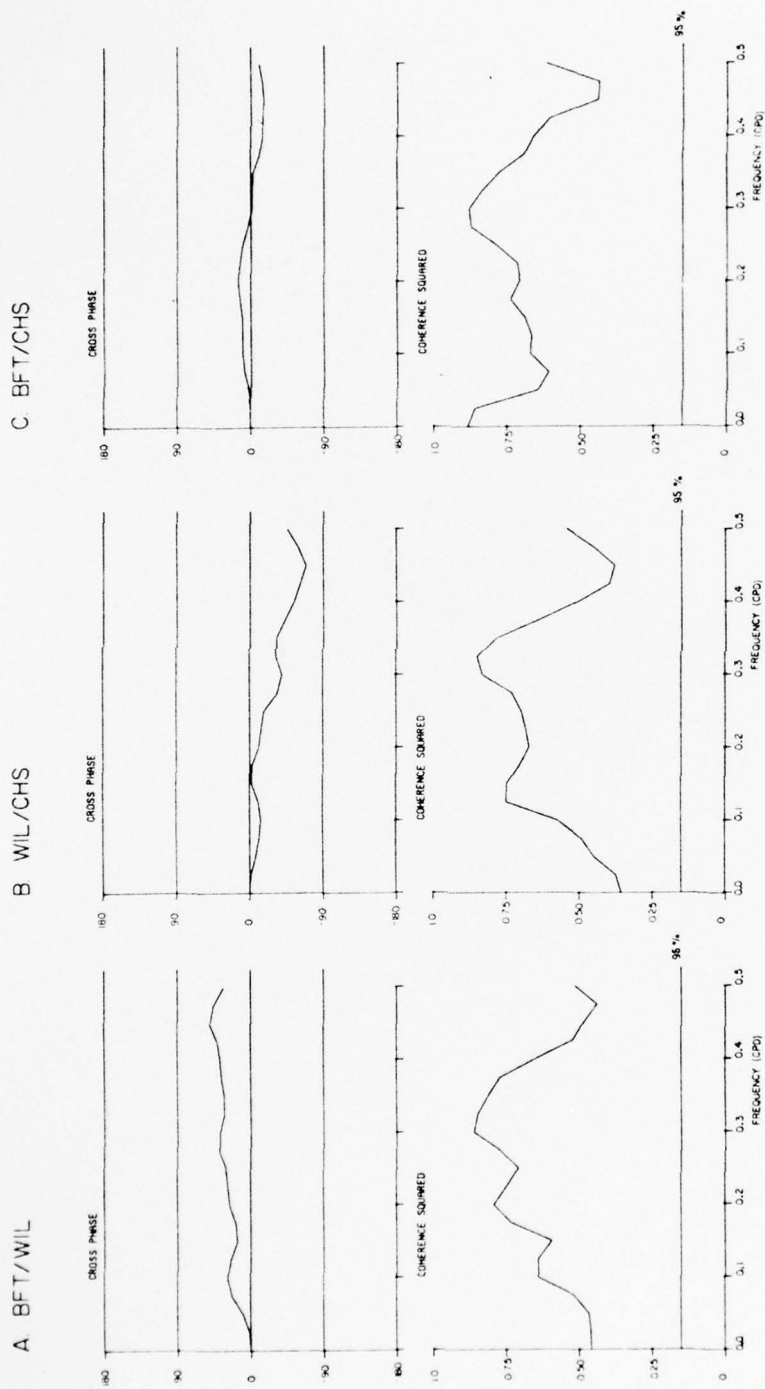


Fig. 12 Coherence and phase for barometerically adjusted 292-day sea level records.

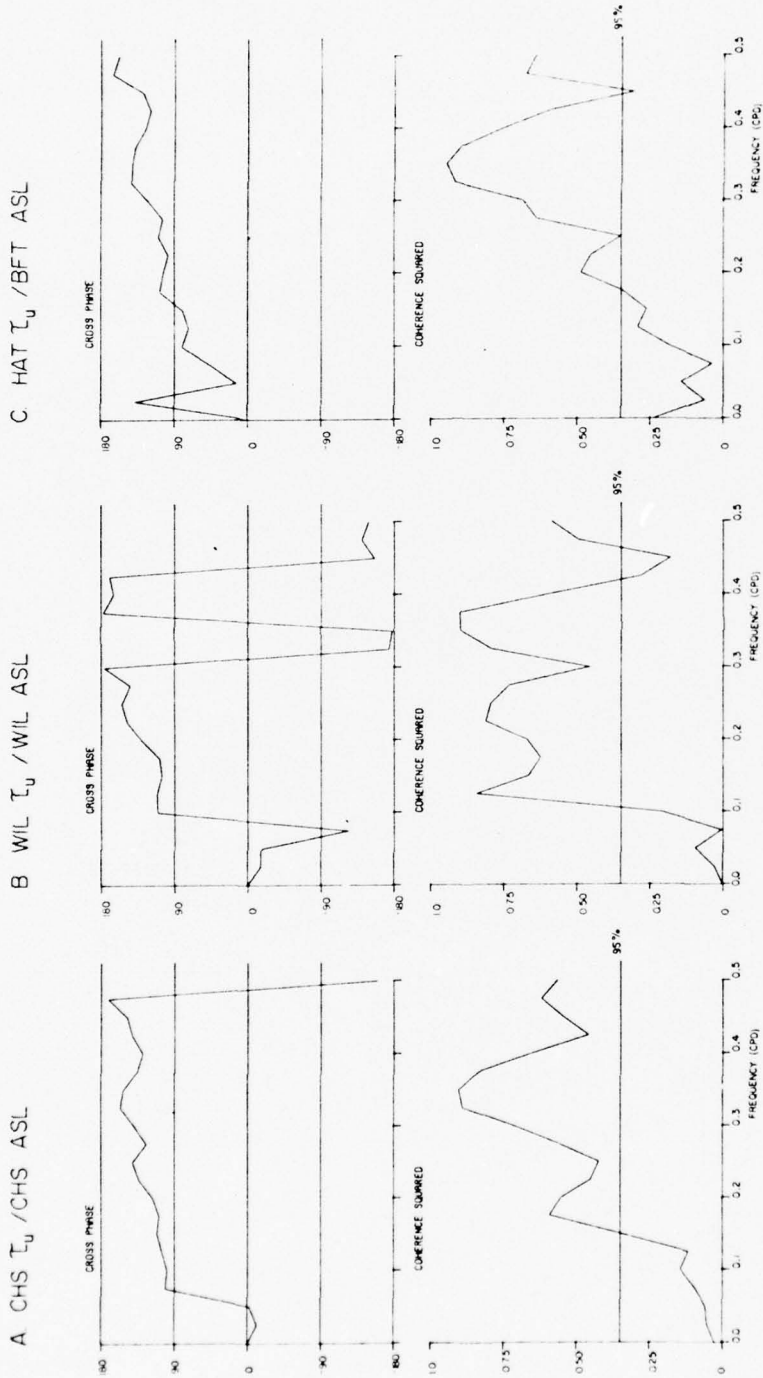


Fig. 13 Coherence and phase for cross shelf wind stress components and barometrically adjusted 120-day sea level records.

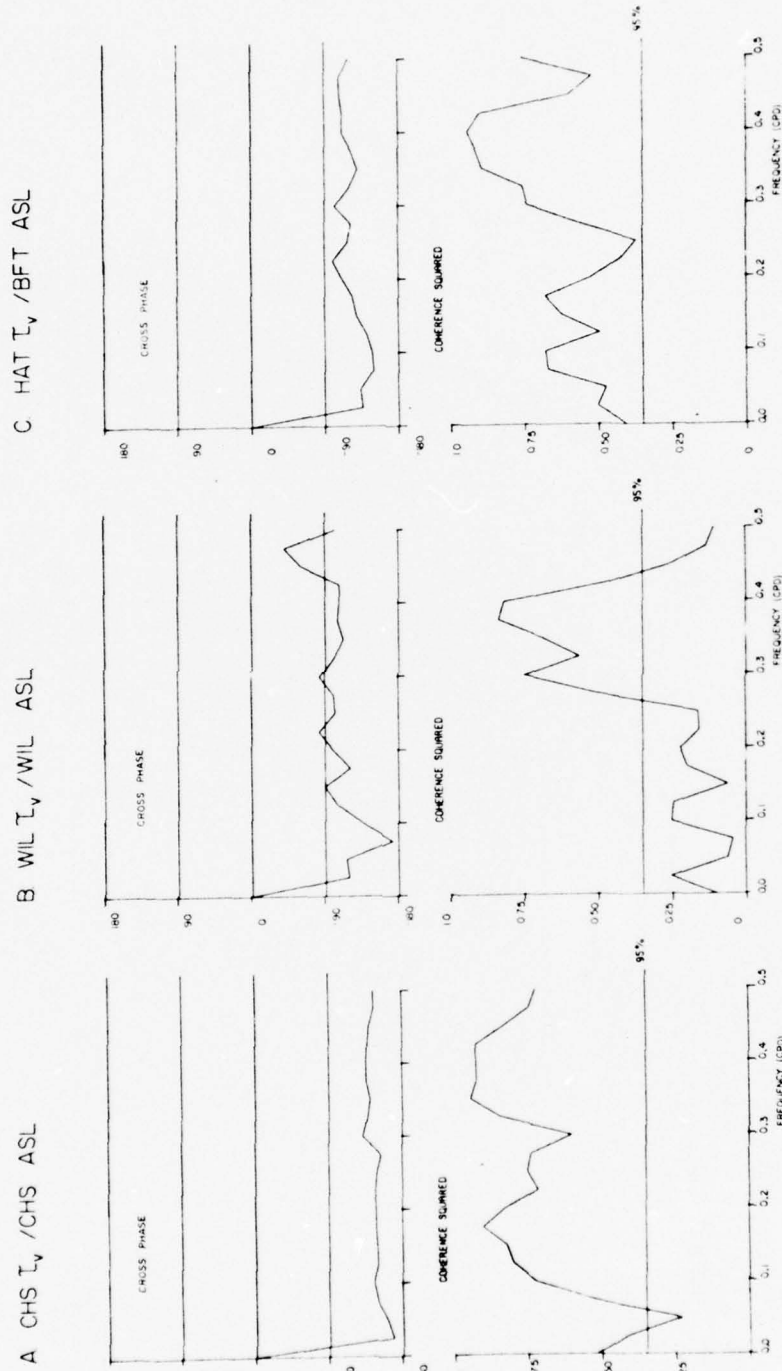


Fig. 14 Coherence and phase for along shelf wind stress components and barometrically adjusted 120-day sea level records.

both components at periods longer than about 10 days, although the case for along shelf wind stress at HAT (Fig. 14C) may be an exception due to the relative exposure of that station to the Mid-Atlantic Bight. The phase relationships generally indicate falling sea level with increasing cross shelf and along shelf wind stress; consistent respectively with coastal sea level set-down due to offshore winds, and with offshore Ekman transport and resultant set-down due to upwelling-favorable northeastward winds.

The emergence of the 2.5 - 3.5 day period band as an important portion of the atmosphere-ocean coupling spectrum indicates a selective forcing of the zero group speed, first mode CSW for the Cape Fear area, which has a period of 3.0 days and a wavelength of 420 km (B76). This CWS is predicted to propagate southward, in opposition to the Gulf Stream, which should produce lagging phases of sea level fluctuations associated with the wave as one proceeds southward along the coast. The phase evidence presented indicates southward propagation from BFT to WIL (the implied wavelength at the 3-day period is 800-1000 km, a factor of two or more larger than predicted), but the phase evidence for southward propagation is at best ambiguous between CHS and the other stations. Additional sea level stations (one or two) located between CHS and WIL would probably resolve the ambiguity. An additional uncertainty concerning direction of phase propagation is introduced by the sheltered, up-river location of the WIL tide gauge. Part of the observed BFT and WIL phase lag may be due to the time required for the disturbance to propagate up the river to the gauge location. However, Mysak and Hamon (1969) also found southward phase propagation in Onslow Bay, confirming the results of this study, using a gauge located at

Southport, near the river mouth. (The Southport tide gauge was not in operation during the period of this study).

In summary, the frequency domain analyses indicate a highly coherent, selective coupling process between the atmosphere and sea level in the 2.5 - 3.5 day band. The sea level fluctuations were also coherent in the 7 - 30 day band, but coupling with atmospheric wind stresses was weaker than in the 2.5 - 3.5 day band. The horizontal coherence scales of atmospheric and sea level fluctuations were much larger than the greatest station spacing in this study (~500 km). The phase calculations suggest southward CSW propagation from BFT to WIL, consistent with Mysak and Hamon's results, but the data considered are too sparse to confirm or contraindicate southward propagation along the coast south of WIL. A study using more closely tide gauges is necessary to clearly resolve the phase propagation direction.

5. Multiple Regression Models

It is clear from the preceding time and frequency domain analyses that sea level fluctuations are coupled with atmospheric forces in preferred frequency bands. Since atmospheric pressure and winds may be correlated with each other to a significant degree in the same frequency bands, it is desirable to correct the transfer function between sea level and a particular atmospheric forcing variable for the coherent contribution of all other included forcing variables. Thus, for example, the transfer function between atmospheric pressure and sea level (the "barometric function") can be corrected linearly in each frequency band to remove the effects of wind stresses that are coherent with the pressure. Failure to recognize correlation between atmospheric forcing variables can cultivate misleading physical models; e.g., that sea level fluctuations in a particular frequency band are entirely forced by pressure fluctuations, when in fact significant forcing may be due to a wind stress component which is highly coherent with the pressure in that band.

The commonly applied static barometric sea level "correction" (cf., Mysak and Hamon, 1969) is based on the premise that at sufficiently low frequencies sea level responds as an "inverse barometer" to changes in pressure (a pressure increase of 1 mb results in a static sea level depression of 1.01 cm). The static correction usually does account for a portion of local sea level fluctuations, but a significant nonbarometric residual correlation often remains, indicating the importance of dynamic as well as static processes (Brooks and Mooers, 1977). The static correction seems to be a helpful first step in exposing dynamic relationships between atmospheric pressure and sea level fluctuations. A more detailed examination

should at least recognize the likely coherence between synoptic-scale atmospheric pressure and wind fluctuations, particularly since CSW's can apparently be forced by either (Mysak, 1967; Adams and Buchwald, 1969).

Sea level fluctuations are considered to be jointly forced by atmospheric pressure and wind stress in the model considered in this section. The linkages between the variables are examined by a multiple-input, linear, frequency-domain regression scheme (Groves and Hannan, 1968). Briefly, the simultaneous regression of an "output" function Y on several "input" functions X_i is carried out in frequency bands by operations performed on the augmented cross spectral matrix containing all combinations of Y and X_i . The ordinary coherence and phase between the output and each input are linearly corrected for the coherent effects of all the other inputs in each frequency band to yield the multiple coherence. The transfer function between the output and each input is likewise corrected for all other coherent inputs. The calculations were carried out with 16 (47) degrees of freedom for the 120 (292) day period. The computer programs used to perform the calculations are part of the NCSU FESTSA time series analysis system (Brooks, 1976b).

Multiple coherence between sea level at BFT and WIL and atmospheric variables is shown in Fig. 15 for 120 and 292 day cases. Each graph shows the coherence increase as pressure (p), offshore wind stress (τ_u) and alongshore wind stress (τ_v) are cumulatively included in the calculation. The horizontal dashed line is the 95% null hypothesis level. The vertical arrows identify the frequencies of the first and second mode, zero group speed CSW's determined for the Cape Fear section (B76). Figure 15 (A and B) also shows the spectrum density for Cape Hatteras atmospheric pressure for the 120 and 292 day period, respectively.

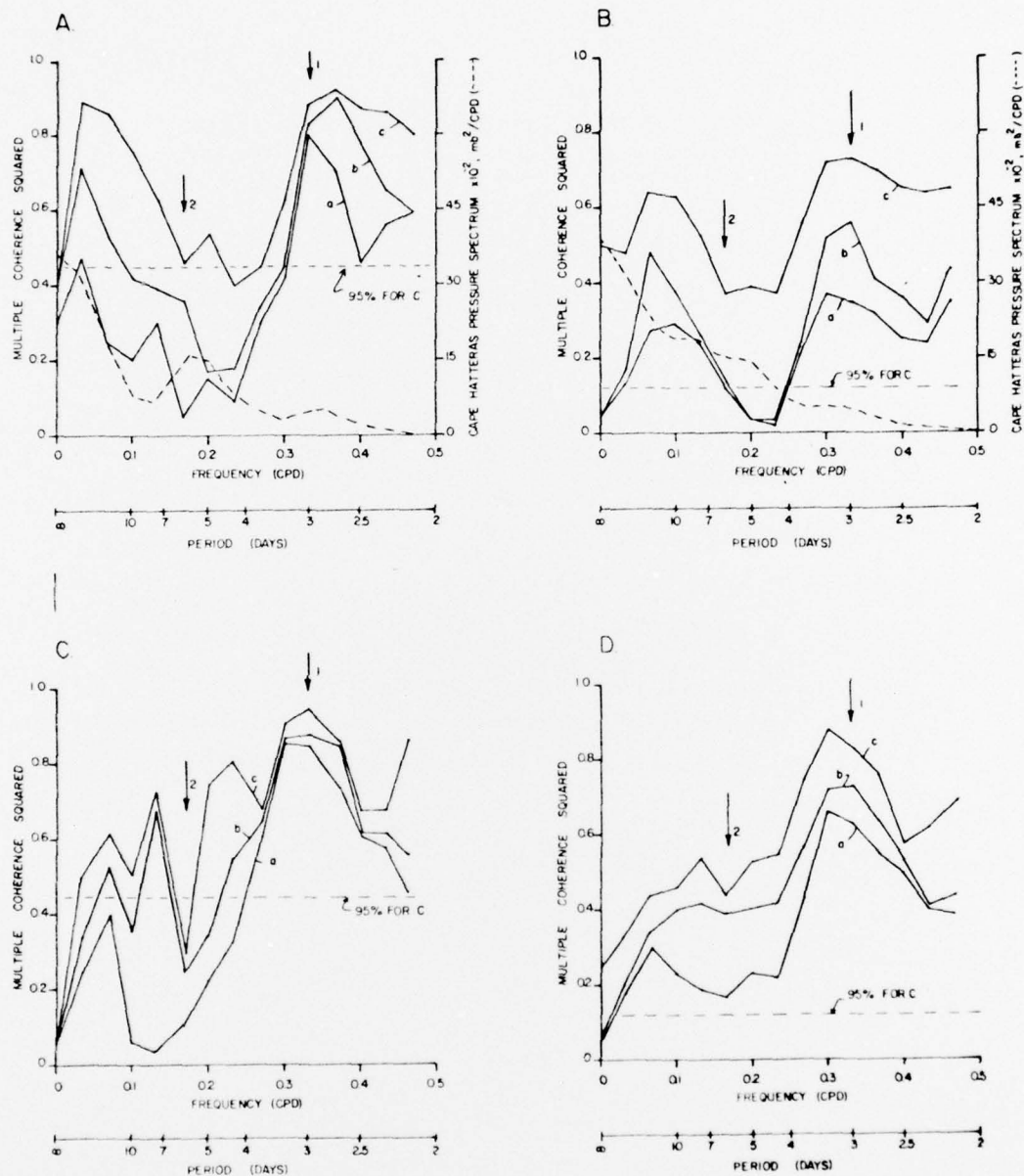


Fig. 15 Multiple coherence between sea level and a) atmospheric pressure, b) pressure and cross shelf wind stress, and c) pressure, cross, and along shelf wind stress for: A) BFT, 120-day record; B) BFT, 292-day record; C) W11, 120-day record; and D) W11, 292-day record. Arrows mark zero group speed frequencies for first and second CSW modes (from Brooks, 1976a). The Cape Hatteras pressure spectrum for 120-day (A) and 292-day (B) cases is shown by the heavy dashed line.

By including the wind stress components, the coherence is increased substantially at both stations and for both record lengths. Coherence peaks are prominent and significant at both stations in period bands of 2.5 to 3.5 days and 7 to 30 days, with the highest coherence value (0.95) occurring at 3.0 days at WIL for the 120 day (winter) record. The 2.5 to 3.5 day band straddles the first mode, zero group speed CSW frequency, suggesting that CSW's are selectively forced in that band. Barotropic CSW's forced in the 7 to 30 day band should exhibit southward phase and group speeds, but it is not suggested by the calculations in B76 that there should be a selective coupling in that band. The 7 to 30 day peak is stronger relative to the 2.5 to 3.5 day peak when only the winter months are included, Fig. 15 A and C, probably reflecting a higher degree of organization of winter atmospheric forcing patterns. The pressure spectra also reflect this difference, with the winter case (Panel A) showing prominent peaks at periods of about 6 days and 3 days; whereas the combined winter and summer case (Panel B) is generally "red," with only hints of peaks in similar bands. The 6-day winter pressure spectrum peak is probably associated with atmospheric cold front passages; the 3 day peak, which is less energetic by a factor of three (but much more strongly coupled to sea level), is probably second harmonic evidence of the impulsive time scale (~1 day) of the pressure and wind disturbances usually associated with a cold front passage over a fixed station (Brooks and Mooers, 1977).

The WIL coherence differs substantially from BFT only in the period band of 7 to 30 days. In this band, the WIL peak is less well defined and indicates relatively less accrual of coherence as the wind stress components are included. The smaller WIL coherence at periods longer than 7 days may occur because the tide gauge is located approximately 35 km upstream from the mouth of the Cape Fear river, in a sheltered location at which exposure

to fluctuations occurring on the shelf offshore may be reduced.

Superbarometric (greater in magnitude than 1.01 cm/mb) sea level responses to pressure fluctuations generally occur in bands of high coherence (Fig. 16). The response is generally sub-barometric in bands of low coherence when the effects of wind stress are included. The uncorrected barometric moduli (X's) at WIL tend to overestimate the corrected moduli for periods shorter than about 4 days; a similar result is not evident at BFT. With the exception of the winter WIL case, the barometric functions generally indicate an out-of-phase relationship between atmospheric pressure and sea level, as expected. Phase estimates are shown only for frequencies at which the 95% confidence interval (which is proportional to the product of the coherence and barometric function modulus) is less than 360° .

Mysak and Hamon (1969) show uncorrected barometric functions, $b(f)$, for Southport (near WIL) and Morehead City (near BFT), for the years 1953 and 1954. Their results, presented as $b(f)$ trajectories in the complex plane with frequency as parameter, are qualitatively consistent with the uncorrected moduli shown in Fig. 16. However, when the coherent wind stresses are included, the curious rotary phase patterns shown by Mysak and Hamon are not reproduced; instead, the corrected phases quite consistently indicate the expected out-of-phase relationship, at least in bands of relatively high coherence. The moduli most strongly modified by inclusion of the wind stresses were those at WIL² for periods shorter than about 4 days. The largest difference between corrected and uncorrected

⁶This may be partially due to shallow water effects, such as wind set-up, in the Cape Fear River.

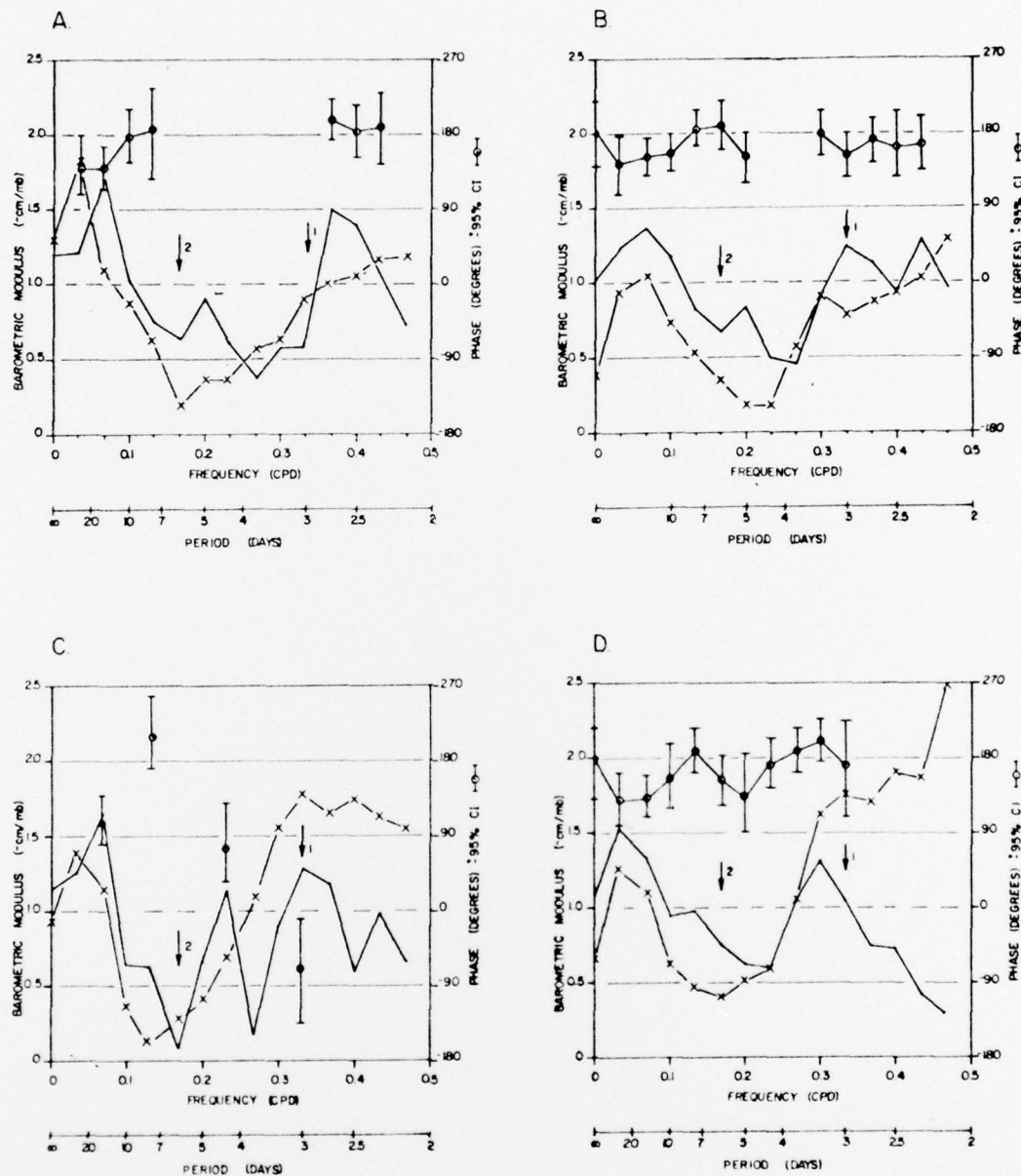


Fig. 16 Barometric function modulus (corrected for coherent wind stress, solid line; uncorrected broken line) and phase for: A) BFT, 120-day record; B) BFT, 292-day record; C) WIL, 120-day record; and D) WIL, 292-day record. Arrows mark zero group speed frequencies of first and second CSW modes (from Brooks, 1976a).

moduli occurred at a period of about 2 days, consistent with Mysak and Hamon's $b(f)$ graphs which show the largest (superbarometric) moduli for periods shorter than 2.5 days.

The corrected superbarometric peaks in Fig. 16 consistently occur in the high coherence bands of Fig. 15, further suggesting dynamic sea level responses to atmospheric forcing in these bands. The ordinary coherence between wind stress and sea level (Figs. 13 and 14) tends to show peaks in the 3 day band, but not at periods longer than 10 days, suggesting that pressure and wind stress fluctuations associated with cold fronts are jointly most effective in forcing sea level fluctuations in the 2.5-3.5 day band.

Sub-barometric sea level responses generally occurred at periods of 4-6 days. These are difficult to explain, particularly in view of the antiphase nature of the response, for one might expect a barometric background function with superimposed dynamic responses in bands where the sea level "admittance" is high; for example, at CSW zero group speed frequencies. It is curious that the smallest moduli occur near the frequency of the most prominent winter pressure spectrum peak⁷, which also corresponds closely to the second CSW mode zero group speed frequency; this suggests strongly preferential excitation of the first CSW mode relative to the second mode.

In summary, the multiple regression model indicates a rather selective coupling mechanism between the atmosphere and sea level in 2.5-3.5 and 7-30 day bands. The 2.5-3.5 day band corresponds well with the first barotropic CSW zero group speed frequency; the winter pressure spectrum

⁷ Mysak and Hamon's smallest $b(f)$ moduli also occurred near a period of 5 days, indicating some measure of stationarity of the process over two decades.

suggests a 3-day period forced by the second harmonic of the pressure field CSW response. The 7-30 day coupling is not clearly explained as a stable, barotropic CSW response. When coherent wind stresses are included, the barometric function generally exhibits the expected 180 degree phase relationship with sea level fluctuations. The barometric moduli also suggest the occurrence of dynamic sea level responses in the 2.5-3.5 and 7-30 day bands.

6. Summary and Conclusions

The most highly coherent sea level-atmospheric coupling occurred in the 2.5 to 3.5 day period band, consistent with an atmospherically-forced, southward propagating continental shelf wave (CSW) expected to occur in this band (Brooks, 1976a). The phase relationships indicated southward propagation from Beaufort to Wilmington in the 2.5 to 3.5 day band, but southward propagation from Wilmington to Charleston was not confirmed.

The multiple coherence between sea level and atmospheric variables also indicates strong coupling in the 2.5 to 3.5 and 7 to 30 day bands. The wind stress components made the least contribution to multiple coherence in the 2.5 to 3.5 day band in the winter season; which suggests that, when coherence between winds and atmospheric pressure are accounted for, the pressure fluctuations provide the primary forcing of sea level fluctuations in this band. For other bands in the winter and for all bands in the joint winter-summer season, addition of the wind stress components significantly increased the multiple coherence. The dominant winter response in the 2.5 to 3.5 day band may be a CSW forced by the second harmonic energy of impulsive pressure and wind stress fluctuations associated with the passage of cold fronts over the area. The sea level response to the fundamental atmospheric pressure oscillation (at a period of about 6 days) was considerably smaller than at the 3 day period, which indicates a strongly preferential excitation of the first CSW mode, compared to the second mode.

The atmospheric pressure-to-sea level transfer functions (the barometric function), when corrected for coherent wind stress effects,

generally indicated the occurrence of dynamic, antiphase sea level responses to pressure fluctuations at periods of 2 to 4 days and greater than 10 days. The static "barometer factor" (-1.01 cm/mb) only crudely approximates the barometric function when averaged over 0 to 0.5 cycles per day, and then only if the coherent wind stresses are included. The uncorrected barometric function at Wilmington substantially over-estimated the corrected one for periods shorter than about 4 days. The curious "rotary" barometric function phases reported by Mysak and Hamon (1969) are not reproduced here when the wind stress components are included in the calculations.

In conclusion, these results indicate that atmospherically forced CSW's contribute to the total circulation of the continental shelf and slope waters off North Carolina. The most important spatial (temporal) scale of motion to be expected solely as a result of atmospherically forced CSW's is about 400 km (3 days); other scales of motion are not excluded. The relative importance of CSW circulation compared to that driven by or associated with other mechanisms (such as, for example, instabilities of the Gulf Stream) remains an open question of great interest.

References

- Adams, J. K. and V. T. Buchwald (1969). The generation of continental shelf waves. Jour. Fluid Mech., 35, 815-826.
- Brooks, D. A. (1976a). Long waves trapped by the Cape Fear continental shelf topography: a model study of their propagation characteristics and circulation patterns. Center for Marine and Coastal Studies Technical Report No. 76(2), North Carolina State University, Raleigh, N. C., July 1976.
- _____ (1976b) Editor. Fast and easy time series analysis at NCSU. Center for Marine and Coastal Studies, North Carolina State University, Raleigh, North Carolina, November 1976.
- _____ and C. N. K. Mooers (1977). Free, stable continental shelf waves in a sheared, barotropic boundary current. Jour. of Geophys. Res., 82, (to appear June 1977).
- Groves, G. W. and E. J. Hannan (1968). Time series regression on sea level. Rev. Geophysics, 6(2), 129-174.
- Hamon, B. V. (1962). The spectrums of mean sea level at Sydney, Coff's Harbor and Lord Howe Island. Jour. of Geophys. Res., 67, 5147-5155.
- Mooers, C. N. K. and R. L. Smith (1968). Continental shelf waves off Oregon. Jour. of Geophys. Res., 74, 549-557.
- Mysak, L. A. (1967). On the very low frequency spectrum of the sea level on a continental shelf. Jour. of Geophys. Res., 72, 3043-3047.
- _____ and B. V. Hamon (1969). Low frequency sea level behaviour and continental shelf waves off North Carolina. Jour. of Geophys. Res., 74, 1397-1405.
- Richardson, W. S., W. Schmitz, Jr., and P. P. Niiler (1969). The velocity structure of the Florida Current from the Straits of Florida to Cape Fear. Deep-Sea Res., 16 (supplement), 225-231.

List of Figure Captions

- Fig. 1 Map of South Atlantic Bight, showing locations of tide gauge and atmospheric station data used in the study.
- Fig. 2 Onslow Bay continental shelf topography, showing coordinate system orientation.
- Fig. 3 Low pass filter energy response envelope function. Attenuation at 1 CPD is 10^6 .
- Fig. 4 Filtered atmospheric pressure at three coastal stations.
- Fig. 5 The filtered along shore wind stress component at three coastal stations.
- Fig. 6 Filtered wind stress vectors in the rotated coordinate system for three coastal stations.
- Fig. 7 Wind stress vectors at Cape Hatteras and their relation to unadjusted (solid lines) and barometrically adjusted (dashed lines) sea level. Static adjustment is accomplished by subtracting 1.01 cm from sea level for each local atmospheric pressure increase of 1 mb.
- Fig. 8 Coherence and phase for atmospheric pressure and wind stress components.
- Fig. 9 Coherence and phase for unadjusted 120-day sea level records.
- Fig. 10 Coherence and phase for unadjusted 292-day sea level records.
- Fig. 11 Coherence and phase for barometrically adjusted 120-day sea level records.
- Fig. 12 Coherence and phase for barometrically adjusted 292-day sea level records.
- Fig. 13 Coherence and phase for cross shelf wind stress components and barometrically adjusted 120-day sea level records.
- Fig. 14 Coherence and phase for along shelf wind stress components and barometrically adjusted 120-day sea level records.
- Fig. 15 Multiple coherence between sea level and a) atmospheric pressure, b) pressure and cross shelf wind stress, and c) pressure, cross, and along shelf wind stress for: A) BFT, 120-day record; B) BFT, 292-day record; C) Wil, 120-day record; and D) WIL, 292-day record. Arrows mark zero group speed frequencies for first and second CSW modes (from Brooks, 1976a). The Cape Hatteras pressure spectrum for 120-day (A) and 292-day (B) cases is shown by the heavy dashed line.

Fig. 16 Barometric function modulus (corrected for coherent wind stress, solid line; uncorrected broken line) and phase for: A) BFT, 120-day record; B) BFT, 292-day record; C) WIL, 120-day record; and O) WIL, 292-day record. Arrows mark zero group speed frequencies of first and second CSW modes (from Brooks, 1976a).

PREVIOUS PUBLICATIONS PUBLISHED
By
THE CENTER FOR MARINE AND COASTAL STUDIES

Wave-Current Force Spectra, C. C. Tung and N. E. Huang, Report No. 72-2,
December, 1972.

A Survey of North Carolina Beach Erosion by Air Photo Methods, H. E.
Wahls, Report No. 73-1, May, 1973.

Sediment Movement in Tubbs Inlet, North Carolina, Robert P. Masterson,
Jr., Jerry L. Machemehl and Victor V. Cavaroc, Jr., Report No. 73-2,
June, 1973.

Influence of Current On Some Statistical Properties of Waves, C. C.
Tung and N. E. Huang, Report No. 73-3, December, 1973.

CTD Sensors, Specific Conductance and the Determination of Salinity,
C. E. Knowles, Report No. 73-3, August, 1973.

Planning for North Carolina's Coastal Inlets - An Analysis of the Pre-
sent Process and Recommendations for the Future, William S. Tilley,
Report No. 73-4, September, 1973.

A Preliminary Study of Storm-Induced Beach Erosion for North Carolina,
C. E. Knowles and Jay Langfelder and Richard McDonald, Report No.
73-5, October, 1973.

A Historical Review of Some of North Carolina's Coastal Inlets, Jay
Langfelder, Tom French, Richard McDonald and Richard Ledbetter,
Report No. 74-1, January, 1974.

Statistical Properties of Kinematics and Dynamics of a Random Gravity
Wave Field, C. C. Tung, Report No. 74-2, June, 1974.

A New Technique of Beach Erosion Control, Tom French, Jerry L.
Machemehl and N. E. Huang, Report No. 74-3, June, 1974.

Citizen Participation in North Carolina's Coastal Area Management
Program, Steve Tilley, Report No. 74-4, June, 1974.

An Experimental Study of Scour Around Marine Foundations Due to
Oscillatory Waves and Unidirectional Currents, Greg N. Abad and
Jerry L. Machemehl, Report No. 74-5, September, 1974.

Proceedings of A Conference on Coastal Management, Report No. 74-6,
September, 1974.

Statistical Properties of Fluid Motion and Fluid Force in A Random
Wave Field, Keikhosrow Pajouhi and C. C. Tung, Report No. 75-1,
May, 1975.

A Numerical Method for Solutions of Systems of Non-Linear Algebraic Equations, John M. Klinck and Leonard J. Pietrafesa, Report No. 75-2, July, 1975.

Wave-Current Interactions in Water of Variable Depths, A. M. Radwan, C. C. Tung and N. E. Huang, Report No. 75-3, August, 1975.

Conference Proceedings Energy From The Oceans Fact or Fantasy?, Jerome Kohl, Report No. 76-1, UNC-SG-76-04, January, 1976.

Long Waves Trapped by the Cape Fear Continental Shelf Topography: A Model Study of Their Propagation Characteristics and Circulation Patterns, David A. Brooks, Report No. 76-2, July, 1976.

A Comparative Study of Three Methods of Inhibiting Scour Around A Vertical Circular Cylinder, David M. Rooney and Jerry L. Machemehl, Report No. 76-3, September, 1976.

A Flow Study of Drum Inlet, North Carolina, Paul R. Blankinship, Report No. 76-4, UNC-SG-76-13, November, 1976.

Dune Stabilization With Panicum amarum Along the North Carolina Coast, E. D. Seneca, W. W. Woodhouse, Jr., and S. W. Broome, Report. 77-1, UNC-SG-77-03, February, 1977.

A Mathematical Model of Nutrient Distribution In Coastal Waters, Eileen E. Hofmann, Leonard J. Pietrafesa, Larry P. Atkinson, Gustav-A. Paffenhöfer and William M. Dunstan, Report No. 77-2, February, 1977.

An Experimental Investigation of Some Combined Flow Sediment Transport Phenomena, Larry Bliven, Norden E. Huang and Gerald S. Janowitz, Report No. 77-3, UNC-SG-77-04, February, 1977.

Thermal Effluent Transport Pathways In Coastal Waters Near The Mouth Of The Cape Fear River Estuary, Leonard J. Pietrafesa, Paul Blankinship and Richard D'Amato, Report No. 77-4, CP&L No. 77-04, March, 1977.

Onslow Bay Physical/Dynamical Experiments Summer-Fall, 1975 Data Report, L. J. Pietrafesa, D. A. Brooks, R. D'Amato and L. P. Atkinson, Report No. 77-5, ERDA Contract No. E(38-1)-902, UNC-SG-77-07, March, 1977.

Sea Level Fluctuations Off The Carolina Coasts And Their Relation To Atmospheric Forcing, David A. Brooks, Report No. 77-6, May, 1977.